J. COMBIN. MATH. COMBIN. COMPUT. 127b (2025) 5149--5164

Journal of Combinatorial Mathematics and Combinatorial Computing
www.combinatorialpress.com/jcmcc

Combinatorial Press

Simulation and optimization of vibration noise of Fe-based soft magnetic composite core reactor based on the finite element method

Yangyang Ma[1], Wenle Song[1], Jie Gao[2,✉], Yang Liu[2], Yilei Shang[2], Weimei Zhao[2], Fuyao Yang[2]

[1] *State Grid Cangzhou Electric Power Supply Company, Cangzhou, Hebei, 061000, China*

[2] *China Electric Power Research Institute, Beijing, 100192, China*

ABSTRACT

Fe-based soft magnetic composites have important applications in reactor core manufacturing due to their superior magnetic properties. In this paper, the vibration noise characteristics of the reactor with core made of this material are investigated and simulated and optimized by finite element method. First, a three-dimensional finite element model of the reactor is established to analyze the electromagnetic force distribution and vibration displacement velocity, and then the accuracy of the finite element analysis model is verified by combining the simulation experimental data. On this basis, the oxidation time parameters of the Fe-based soft magnetic composite material are adjusted, and the optimal parameters are selected to improve the vibration of the reactor, so as to achieve the purpose of improving the working condition of the reactor. The results show that the magnetic loss and other properties of the material have an important influence on the core vibration, and the reasonable optimization of the composite material structure parameters can reduce the vibration amplitude of the reactor and effectively suppress the noise. This study provides a theoretical basis for the design and optimization of this type of reactor.

Keywords: finite element model, vibration displacement velocity, Fe-based soft magnetic composite material, core reactor

1. Introduction

Dry-type core reactors are mainly used to compensate the capacitive currents on the high-voltage side, the low-voltage side in long-distance transmission lines and substations to maintain voltage stability [1-2]. In order to avoid excessive capacitive currents causing overvoltage in the grid and leading to reactor insulation defects, reactors are now widely used in urban distribution networks for reactive power compensation to reduce the insulation requirements and investment in the power system [3-

✉ Corresponding author.
E-mail address: conch3501@163.com (J. Gao).
Received 12 January 2024; Revised 05 March 2024; Accepted 25 December 2024; Published Online 16 April 2025.
DOI: 10.61091/jcmcc127b-286

4]. The traditional silicon steel core reactor is noisy and has a long propagation distance, and the noise-induced nuisance problem is getting more and more attention [5].

With the expansion of China's power grid construction scale and the continuous improvement of industrial requirements for electrical equipment, reactor, as an important reactive power compensation device in the power grid, has the functions of ensuring the balance of reactive power in the power system, limiting the short-circuit current, suppressing the line over-voltage and over-current, balancing the impact of impact loads on the power grid, and reducing the line losses [6-8]. However, the vibration noise problem of reactor in the operation process is more serious, which not only interferes with the normal life of the surrounding residents, but also exacerbates the aging damage of the reactor itself, and even makes the power grid to produce more serious safety accidents [9-10]. Iron core reactor due to the special core structure and electromagnetic, mechanical and other physical fields together lead to its vibration in the operation process is more serious, which has become one of the factors that limit its development [11-12]. Thus, it is necessary to comprehensively calculate and analyze the electromagnetic vibration of the core reactor, which is of great significance to further reduce the vibration noise of the reactor [13-14].

In this paper, based on the electromagnetic field characteristics of the core reactor and Maxwell's differential equations, a three-dimensional finite element analysis model of Fe-based soft magnetic composite core reactor is established in ANSYS Maxwell software environment. According to Maxwell's system of equations, such as Faraday's law of electromagnetic induction, we propose a method of analyzing the magnetic field distribution of the core reactor, based on which we combine the Lorentz force to construct a method of calculating the vibration displacement of the core reactor. In this study, the Fe-based soft magnetic composite core reactor is selected as the simulation object, and the accuracy of the three-dimensional finite element simulation model applied in the experiment is verified by comparing the simulation results with the measured results. Then we take the oxidation time as the main analysis parameter, simulate and analyze the performance of Fe-based soft magnetic composites under different parameters, and investigate the influence and optimization effect of different oxidation parameters of Fe-based soft magnetic composites on the vibration of the core reactor.

2. Methods for determining the properties of Fe-based soft magnetic composites

The performance tests of Fe-based soft magnetic composites include a density tester to test the true density of the powder, Archimedes' drainage method to test the density of the soft magnetic composite material, a four-point probe to test the resistivity, an impedance analyzer to test the inductance, an $B-H$ -analyzer to measure the magnetic loss, and a VSM analyzer to test the saturated magnetization strength and coercivity. The test equipment all meets the test requirements.

2.1. Density testing

The density measurements of the experimental raw materials and prepared soft magnetic composite powders were performed using a Micromeritics AccuPyc1330 true density tester (Mac Instruments, USA).

The relative density of the prepared soft magnetic composites was tested using the Archimedes drainage method at a testing temperature of 25°C, and the average value was taken after three tests, and the formula was calculated as follows:

$$\rho_{\text{Sample}} = \frac{\rho_0 m_1}{m_1 - m_2} \tag{1}$$

Where ρ_{Sample} is the measured density of the soft magnetic composite $\left(g/cm^3\right)$, ρ_0 is the density of anhydrous ethanol at 25°C $\left(g/cm^3\right)$, m_1 is the mass of the soft magnetic composite in air (g), m_2 is the mass of the soft magnetic composite in anhydrous ethanol (g).

2.2. *Resistivity testing*

Resistivity is one of the important physical parameters for evaluating the performance of soft magnetic composites. In this experiment, the resistivity was obtained by testing the surface resistivity of the polished surface of soft magnetic composites using a four-point probe tester (RTS-8). Three sets of resistivities on each of the upper and lower surfaces of the material were tested and averaged to minimize the error.

2.3. *Magnetic permeability test*

In this experiment, the inductance value (L) and quality factor (Q) are determined by LCR tester (IM3570A988-06, HIOKI, Japan), and in order to reduce the error of the test during the test as much as possible copper enameled wire coils are wound around the samples, and the winding coil in this experiment is 20 turns, and the test voltage is 0.3 V. The inductance value of soft magnetic composites is calculated through the test, and the permeability of the preparation is calculated (μ), which is calculated by the following formula:

$$\mu = \frac{lL}{\mu_0 N^2 A} \tag{2}$$

where l is the effective magnetic circuit length of the soft magnetic composite (m), A is the effective cross-sectional area of the soft magnetic composite $\left(m^2\right)$, N is the number of turns of the wound copper enameled wire, and μ_0 is the vacuum permeability $\left(4\pi\cdot 10^{-7} H/m\right)$.

2.4. *Static magnetic properties and magnetic loss tests*

The saturation magnetization strength and coercivity are tested by using a static magnetic properties measuring instrument, Vibrating Sample Magnetometer (VSM) [15], which has a high sensitivity and allows direct reading of the magnitude of the values. In this experiment, the static magnetic properties of the material are tested by using the Vibration Sample Magnetometer (VSM) type 7404 manufactured by LakeShore, USA.

In this experiment, the total magnetic loss of different flux densities and different frequencies is tested, and the change rule is investigated. According to the shape of the prepared soft magnetic composites, the total magnetic loss of the soft magnetic composites [16] was measured by $B-H$ analyzer (SY-8219, Iwasaki, Japan) at room temperature.

3. Finite element modeling and analysis of core reactors

3.1. *Three-dimensional simulation model construction based on ANSYS Maxwell*

3.1.1. ANSYS Maxwell software fundamentals. ANSYS Maxwell [17] is a software based on Maxwell's differential equations in the form of finite element discretization, which transforms electromagnetic field problems in engineering into matrix solutions, with the advantages of ease of use, power, and accuracy of results. The software consists of modules for electrostatic field, static magnetic field, time-varying electric field, time-varying magnetic field, eddy current field, transient field and temperature field calculations, etc. It is usually used in the field of electrical engineering to analyze the static, dynamic, normal and faulty conditions of electromagnetic devices such as electric motors, transformers, and permanent magnet devices. With excellent wizard user interface, high-precision adaptive profiling technology, user-definable material library and powerful post-processing functions, it is widely used by engineering designers and research scholars.

Maxwell is a software package that enables human-computer interaction to analyze electromagnetic field problems in two or three dimensions using finite element analysis methods. Depending on the model built, Maxwell can calculate both electric and magnetic fields, as well as specific physical quantities such as force, torque, inductance, capacitance or power loss. Maxwell can also plot various types of fields such as vector magnetic potential, magnetic field strength, magnetic induction strength, electric density, and energy. The ANSYS Maxwell 3D EM analysis module includes a static magnetic field solver, eddy current field solver, axial magnetic field eddy current solver, electrostatic field solver, constant electric field solver, alternating electric field solver, transient solver, temperature field solver, and parametric analyzer The following are some of the most common parameter analyzers.

3.1.2. Three-dimensional finite element modeling process. Under the condition that the structure, material, voltage level and capacity of the magnetron reactor are known, the magnetron reactor ontology is created in ANSYS Maxwell software for calculation and analysis.

1) Create project. Start the Maxwell program, enter the Maxwell 3D modeling simulation environment, generate a new project file, rename it mcr. Next, execute the menu command Maxwell 3D/Solution Type, set the solution type to Transient.

2) Draw the geometric model. Execute Modeler/Units, set the unit as mm, execute Maxwell 3D/Model/Set Model Depth, set the core length, and draw the geometric model of the core and winding of the magnetron reactor. Set the center point, determine the coordinates of the key points of each component according to the length, and then use Boolean operation and mirror operation to get the complete geometric model of the core reactor.

3) Setting Material Properties. Maxwell material library mainly consists of two categories, one is the common material library for 3D finite element calculation that comes with the system; the other is the user material library, which allows individuals to add their own materials in the library according to the actual material selection. For customized nonlinear materials, you need to add the B-H curve of nonlinear materials.

4) Setting boundary conditions. Select each segment of the air gap border and set it as a balloon boundary condition, named Balloon1.

5) Set the winding and excitation conditions. Winding setup, select the winding, right-click and choose Assign Excitation/Coil, set the winding polarity and winding turns. Add winding and set excitation source, click Excitation/Add Winding, click Winding/Add Coil, add the winding to the corresponding excitation. Setting the excitation source, there are three main excitation methods in Maxwell, voltage source, current source and applied circuit. In this paper, we use ANSYS Maxwell and Simplorer joint simulation method, so we set up the applied excitation circuit in Simplorer, and then import the reactor body computational analysis model into Simplorer.

6) Setting of Segmentation Parameters. It is necessary to set the corresponding sectioning for each structural part of the model, click Assign Mesh operation/On Selection/Length Based, name the corresponding parts, set Lengthof Elements, Number of Elements. If the result does not meet the requirements, you can change the parameters and re-do the dissection.

7) Setting solving parameters. Click Maxwell 3D/Analysis Setup/Add Solution Setup in the menu bar to set the solution parameters such as Stop time, Time Step and Name. Follow the steps to complete the construction of the ontology model, click Maxwell 3D/Validation Check on the menu bar after all the parameters are set up to carry out self-checking of the model, and click Maxwell 3D/Analyze All after checking that there is no error in the parameters and operations of each step, and then the model will start to carry out ontology calculation and analysis. After the analysis is complete, select all parts

of the model and click Maxwell 3D/Fields to view various types of field diagrams in the Fields list, such as vector magnetic potential, magnetic field strength, magnetic induction strength, electric density, energy, other field quantities and user-defined field quantities.

3.2. Reactor vibration analysis

3.2.1. Principles of Finite Element Calculation of Electromagnetic Forces. In the calculation of the electromagnetic force problem of the core reactor, the basic laws of electromagnetic phenomena can be expressed by Maxwell's system of equations, and the finite element method is no exception, Maxwell's system of equations [18] contains four laws are Ampere's loop law, Faraday's law of electromagnetic induction, Gauss's law of flux and Gauss's law of flux, and the system of equations contains four variables and two source quantities, which are expressed in differential form as follows:

$$\nabla\times\bar{H}=\bar{J}+\sigma\frac{\partial\bar{D}}{\partial t} \tag{3}$$

$$\nabla\times\bar{E}=-\frac{\partial\bar{B}}{\partial t} \tag{4}$$

$$\nabla\cdot\bar{B}=0 \tag{5}$$

$$\nabla\cdot\bar{D}=\rho \tag{6}$$

Where, H is the magnetic field strength, E is the induced electric field strength, B is the magnetic induction strength, J is the applied current density, D is the potential shift vector, and σ is the conductivity.

Since the frequency of the reactor electromagnetic field change is low and the distance between the electromagnetic field source point and the field point is much smaller than the wavelength of the electromagnetic wave in the study of the Fe-based soft magnetic composite core reactor, the calculation of the electromagnetic force of the reactor can be reduced to the problem of the seemingly stable electromagnetic field as shown below:

$$\nabla\times\bar{H}=\bar{J} \tag{7}$$

$$\nabla\cdot\bar{D}=0 \tag{8}$$

When solving the Fe-based soft magnetic composite core reactor again, the composition equation of the medium is also key to the calculation, and for the reactor studied in this paper, the material is an isotropic medium with the composition equation:

$$\bar{B}=\mu\bar{H}=\mu_r\mu_0\bar{H} \tag{9}$$

$$\vec{J}=\sigma\bar{E} \tag{10}$$

Where μ and μ_r are the magnetic permeability and relative magnetic permeability respectively, and μ_0 is the vacuum magnetic permeability with a value of $4\pi\times10^{-7}\ N/A$.

The finite element method for solving the electromagnetic force problem is based on Maxwell's system of equations as the basic theory for analyzing and calculating the magnetic field problem, and the essence of the search is to solve the partial differential equations with the vector magnetic potential as the unknown quantity of the system of equations. In this paper, the magnetic field module in COMSOL is used in the calculation of the magnetic field, and the main dependent variable of its solution is the magnetic vector potential A, and the solution domain equation is:

$$\sigma\frac{\partial A}{\partial t}+\nabla\times\left(\mu_0^{-1}\mu_r^{-1}\nabla\times A\right)=J_e \tag{11}$$

$$\bar{B}=\mu_0\mu_r\bar{H}=\nabla\times A \tag{12}$$

$$J_e=\frac{NI}{S} \tag{13}$$

where B is the magnetic induction, H is the magnetic field strength, J_e is the external current density, N is the number of coil turns, S is the coil cross-sectional area, and I is the coil current.

By comparing and analyzing the analytical method and the finite element method, it can be seen that although the analytical method is widely used in the electromagnetic force calculation of the reactor, it is not convenient to use the results of the electromagnetic force distribution calculated by the analytical method to analyze the loss, temperature field and stress field. At the same time in the calculation of magnetic field, the analytical method is very complex calculation process involves a lot of parameters, and the solution results can not directly observe the distribution of the magnetic field, is not conducive to the analysis of the distribution of magnetic field inside and outside the reactor, so this paper uses the finite element method to calculate and analyze the magnetic field of Fe-based soft magnetic composite material core reactor.

3.2.2. Vibration Displacement Calculation Methods. The method used in calculating the electromagnetic force in the Fe-based soft magnetic composite core reactor is the Lorentz force method. The essence of the Lorentz force is the force of the magnetic field on the electric current. The Lorentz force method [19] is the calculation of the force exerted on each current-carrying microelement, which is given in Eq:

$$dF=idl\times B \tag{14}$$

where i is the current flowing through the coil, B is the magnetic field strength of the coil, and dF is the electromagnetic force per unit length of the coil.

The combined force applied to an object in a magnetic field can be calculated by integrating the force for each current-carrying microelement:

$$F_v=\int_v(\vec{J}\times\vec{B})dv \tag{15}$$

Where $\vec{J}\times\vec{B}$ is the force density of the conductor, the magnetic field strength B and current density J can be calculated by the calculation of the magnetic field.

When the Fe-based soft magnetic composite core reactor is in normal operation, the current will flow through the inner coil of the package, and the charged coil will be subjected to electromagnetic force in the alternating magnetic field, which will form the vibration of the reactor's windings, thus generating displacements and deformations. From Ampere's law, it can be seen that the electromagnetic force on the winding is related to three variables, and since the model of the reactor is fixed, the other two variables are generally considered in the calculation of the electromagnetic force, which is proportional to the product of the magnetic induction and the winding current, and proportional to the square of the current, as shown in equation (16):

$$F\propto B\times I\propto I^2 \tag{16}$$

1) When a single frequency current $i(t)=A\sin(2\pi ft)$ is passed:

$$i^2(t)=[A\sin(2\pi ft)]^2=\frac{1}{2}A^2[1-\cos(2\pi\times 2ft)] \tag{17}$$

At this point, the frequency of the electromagnetic force to which the reactor is subjected during operation is not the frequency of the single-frequency current, but is two times the frequency f of the loaded current.

2) When a combined current $i(t)=A_1\sin\left(2\pi f_1t\right)+A_2\sin\left(2\pi f_2t\right)$ containing two frequencies is passed, note $i_1(t)=A_1\sin\left(2\pi f_1t\right)$ and $i_2(t)=A_2\sin\left(2\pi f_2t\right)$:

$$i_1^2(t) = \left[A_1 \sin\left(2\pi f_1 t\right)\right]^2 = \frac{1}{2} A_1^2 \left[1 - \cos\left(2\pi \times f_1 t\right)\right] \tag{18}$$

$$i_2^2(t) = \left[A_2 \sin\left(2\pi f_2 t\right)\right]^2 = \frac{1}{2} A_2^2 \left[1 - \cos\left(2\pi \times f_2 t\right)\right] \tag{19}$$

$$\begin{aligned} i_1(t) i_2(t) &= A_1 \sin\left(2\pi f_1 t\right) A_2 \sin\left(2\pi f_2 t\right) \\ &= \frac{1}{2} A_1 A_2 \left\{\cos\left[2\pi\left(f_1 + f_2\right)t\right]\right\} - \cos\left[2\pi\left(f_1 - f_2\right)t\right] \end{aligned} \tag{20}$$

At this time, the reactor is subjected to four kinds of electromagnetic force during operation, respectively, $i_1(t)$, $i_2(t)$ when acting alone, the frequency of $2f_1$, $2f_2$ electromagnetic force, and $i_1(t)$, $i_2(t)$ combination of current interaction generated by the frequency of $f_1 + f_2$, $\left|f_1 - f_2\right|$ electromagnetic force.

3) When a combined current $i(t) = A_1 \sin\left(2\pi f_1 t\right) + A_2 \sin\left(2\pi f_2 t\right) + A_3 \sin\left(2\pi f_3 t\right)$ containing three frequencies is passed, note $i_1^2(t) = A_1 \sin\left(2\pi f_1 t\right)$, $i_2(t) = A_2 \sin\left(2\pi f_2 t\right)$, $i_3(t) = A_3 \sin\left(2\pi f_3 t\right)$:

$$i_1^2(t) = \left[A_1 \sin\left(2\pi f_1 t\right)\right]^2 = \frac{1}{2} A_1^2 \left[1 - \cos\left(2\pi \times f_1 t\right)\right] \tag{21}$$

$$i_2^2(t) = \left[A_2 \sin\left(2\pi f_2 t\right)\right]^2 = \frac{1}{2} A_2^2 \left[1 - \cos\left(2\pi \times f_2 t\right)\right] \tag{22}$$

$$i_3^2(t) = \left[A_3 \sin\left(2\pi f_3 t\right)\right]^2 = \frac{1}{2} A_3^2 \left[1 - \cos\left(2\pi \times f_3 t\right)\right] \tag{23}$$

$$\begin{aligned} i_1(t) i_2(t) &= A_1 \sin\left(2\pi f_1 t\right) A_2 \sin\left(2\pi f_2 t\right) \\ &= \frac{1}{2} A_1 A_2 \left\{\cos\left[2\pi\left(f_1 + f_2\right)t\right]\right\} - \cos\left[2\pi\left(f_1 - f_2\right)t\right] \end{aligned} \tag{24}$$

$$\begin{aligned} i_1(t) i_3(t) &= A_1 \sin\left(2\pi f_1 t\right) A_3 \sin\left(2\pi f_3 t\right) \\ &= \frac{1}{2} A_1 A_3 \left\{\cos\left[2\pi\left(f_1 + f_3\right)t\right]\right\} - \cos\left[2\pi\left(f_1 - f_3\right)t\right] \end{aligned} \tag{25}$$

$$\begin{aligned} i_3(t) i_2(t) &= A_3 \sin\left(2\pi f_3 t\right) A_2 \sin\left(2\pi f_2 t\right) \\ &= \frac{1}{2} A_3 A_2 \left\{\cos\left[2\pi\left(\left|f_3 + f_2\right|\right)t\right]\right\} - \cos\left[2\pi\left(f_3 - f_2\right)t\right] \end{aligned} \tag{26}$$

Electromagnetic force not only $i_1(t)$, $i_2(t)$, $i_3(t)$ alone when the electromagnetic force generated by the frequency of $2f_1$, $2f_2$, $2f_3$, and there are two frequencies of human interaction with the current frequency of $f_1 + f_2$, $\left|f_1 - f_2\right|$, $f_1 + f_3$, $\left|f_1 - f_3\right|$, $f_3 + f_2$, $\left|f_3 - f_2\right|$ of the electromagnetic force.

Fe-based soft magnetic composite core reactor in the operation of the current in the harmonic component of the more, which constitutes the electromagnetic force of the frequency of the number of more, when the electromagnetic force of the frequency of the number of too much it is easy and the reactor's intrinsic frequency overlap, it is easier to make the various parts of the reactor vibration, when the reactor package inside the windings are subjected to electromagnetic vibration, it will produce a displacement affecting the reactor other parts of the displacement also occurs. When the displacement reaches a certain degree, it will make a part of the reactor deformation.

4. Core reactor vibration noise simulation optimization analysis

4.1. Finite element model simulation accuracy verification

4.1.1. Simulation experiment setup. In order to verify the accuracy of the simulation results of the three-dimensional finite element analysis model of the reactor, the surrounding noise of the Fe-based soft magnetic composite core reactor is measured at an excitation voltage of 1.0Um, and the simulation results are analyzed for accuracy verification. The measured Fe-based soft magnetic composite core reactor has a contour line distance of d=0.5m, a measurement height of 1/3 times the height of the reactor, which is about 1.8m, and an oxidation time parameter of 0h for the preparation of Fe-based soft magnetic composite materials.In the vibration noise simulation test measurements, the measurement points on the contour line are selected at equal intervals for the noise measurement recordings, and since the model in this paper does not take the fan into account, the reactor is selected as the four Measurement points (vibration measurement points 1-4 are the core, clamps, nuts and windings, respectively) are verified. The measurements were performed using a Japanese Riin NL-52 portable noise tester, which has an optional sampling frequency of 12/24/48 kHz, and can meet the needs of vibration and noise simulation testing of Fe-based soft magnetic composite material core reactors.

4.1.2. Analysis of Reactor Vibration Measurement Results. Low-pass filtering is used to reduce noise in the vibration measurement data of Fe-based soft magnetic composite core reactor, and the cutoff frequency is set to 500 Hz to obtain the vibration velocity change curves at each measurement point as shown in Fig. 1, and (a)-(d) represent the results of the vibration velocity analysis of the measurement points 1, 2, 3 and 4, respectively. The test results show that the vibration velocity of each vibration point decreases gradually in the order of core, clamp, nut and winding, and the highest vibration velocities of the four measurement points are 1.50mm/s, 1.08mm/s, 0.67mm/s and 0.62mm/s, respectively.

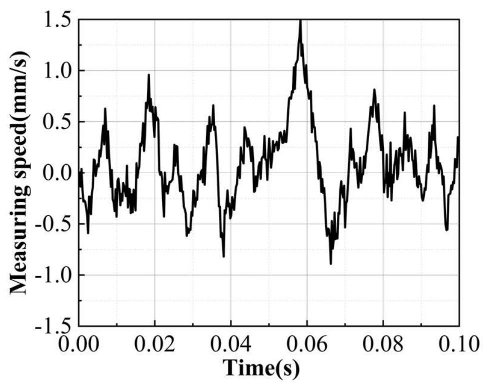

(a) Point 1

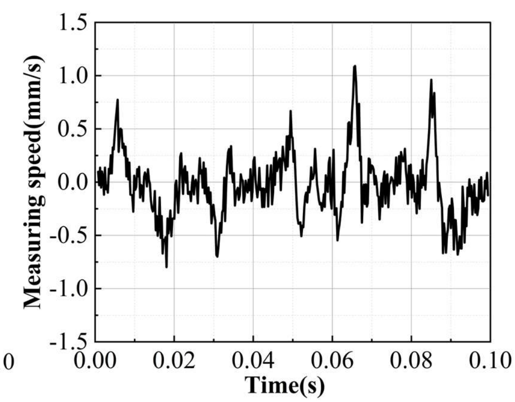

(b) Point 2

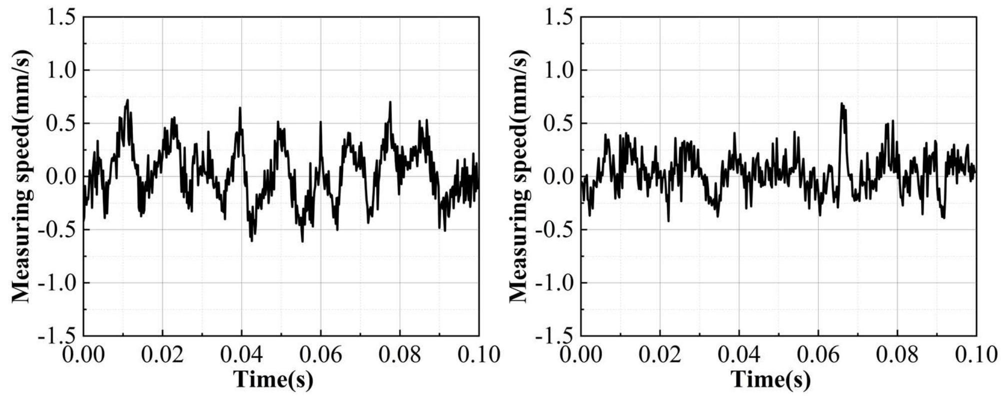

(c) Point 3 (d) Point 4

Fig. 1. Analysis of time domain waveform of measuring vibration velocity

In order to further verify the accuracy of the simulation analysis, with reference to the direction of the test measurement, extract the direction component data of the vibration velocity simulation results of the core, clamps, windings of the three sampling points, and draw the component waveforms of the vibration velocity of each sampling point within 0~0.04s as shown in Figure 2. Comparison of Fig. 1 and Fig. 2 waveforms can be seen, the sampling point simulation results and the measured results of the peak of the time domain waveform and the law of change is relatively close to the amplitude of the vibration speed is basically in the ± 1.2mm / s. The difference between the two and the reason for this is mainly reflected in the vibration speed of the sampling point simulation results. The difference between the two and the reason is mainly reflected in the actual operation of the current changes and field installation methods, etc., the field measured time domain waveform data of the periodicity is slightly worse than the simulation results, in some moments prone to numerical value of the sudden increase in the situation. For the equipment in operation, the contact between the various groups of components and the aging of materials is more complex, and the force and vibration transmission between the various groups of components there are strong nonlinear factors, while the simulation analysis of the situation is relatively ideal, resulting in the simulation results of the periodicity of the more obvious.

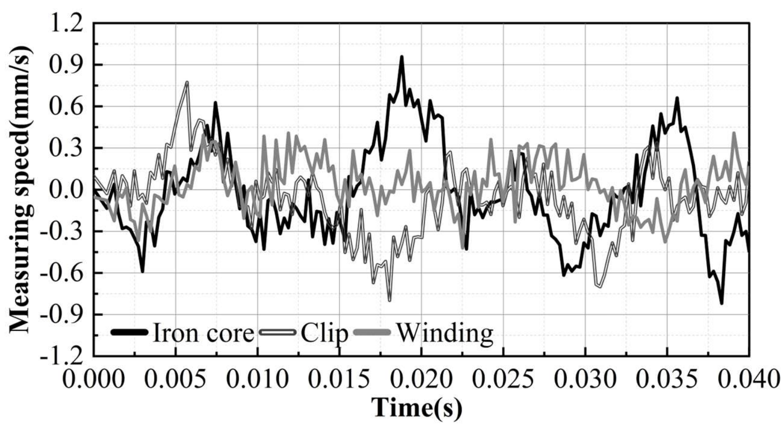

Fig. 2. Time domain waveform of the sample point vibration velocity component

The vibration signals of each vibration point are Fourier transformed to obtain the frequency domain distribution characteristics of the vibration velocity of the reactor, and the analytical results are shown in Fig. 3, with (a) and (b) representing the simulation results and the measured results, respectively. Comparing the measured and simulated results of the reactor vibration, it can be seen that the main vibration frequency of the two is consistent and the relative error of amplitude is less than 5%, and the average relative error is 2.42%, which verifies the accuracy and feasibility of the three-dimensional finite element simulation model. According to the vibration mechanism of the reactor, without considering the nonlinear characteristics of the material, its vibration frequency is determined by the operating current frequency, and should be mainly concentrated in about 100Hz, such as the distribution of vibration frequency of the winding in Figure 3. The vibration frequency of the core and clamping parts is dominated by 100 Hz and its octave frequency, and the vibration frequency of 300 Hz (the simulated vibration speed is 0.257 mm/s and 0.216 mm/s, respectively) is the most significant. This is mainly related to the nonlinearity of the parameters of the Fe-based soft magnetic composite material and the three-phase three-column core structure, which determine the intrinsic modal characteristics of the reactor. In addition, the increase in the 200 Hz component of the clip vibration is due to the superposition of the core and the windings. It can be seen that due to the effect of nonlinear superposition of the three electromagnetic forces and the modal structural properties of the Fe-based soft magnetic composite core reactor, the vibration excitation of the reactor exists in multi-frequency components and is dominated by 100 Hz, 200 Hz, and 300 Hz.

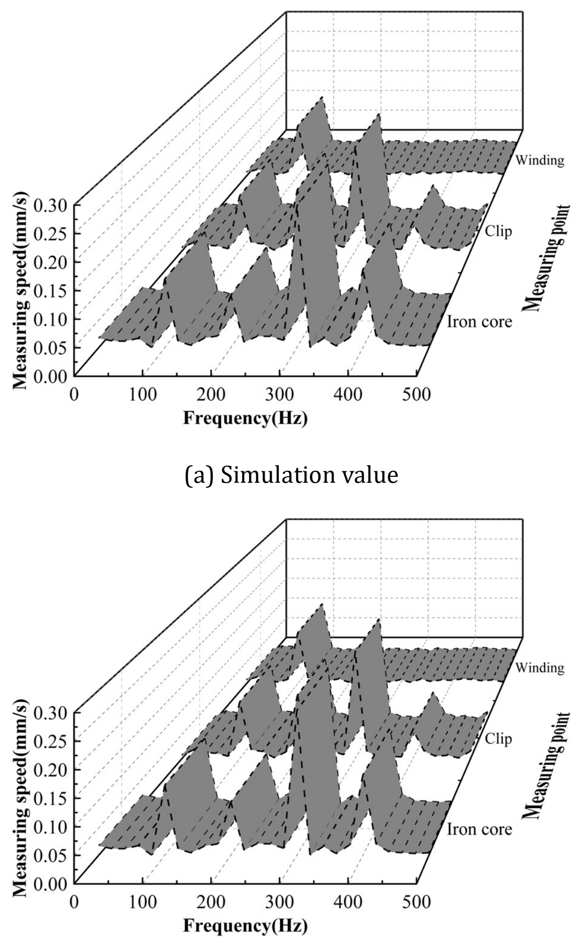

(a) Simulation value

(b) Measured value

Fig. 3. The measured results are compared with the simulation results

4.2. Performance analysis of Fe-based soft magnetic composites under different parameters

Different oxidation times have a large impact on the properties of Fe-based soft magnetic composites, so the oxidation time is used as a parameter to optimize the properties of this material in this study. The results of static magnetic properties analysis of Fe-based soft magnetic composites under different oxidation times are shown in Fig. 4. With the increase of oxidation time, the saturation magnetization strength of the loaded material shows a decreasing trend as a whole, and the magnetization strength of the material is 194.78emu/g and 161.43emu/g at the oxidation time of 0h and 8h, respectively. This is due to the fact that the magnitude of the saturation magnetization strength is mainly related to the type and content of the magnetic particles, and the increase of the oxidation time leads to the thickening of the insulating layer of Fe-based soft magnetic composites, and therefore The non-magnetic phase content of Fe-based soft magnetic composites gradually increases, leading to a continuous decrease in the saturation magnetization strength. At the same time, it will increase the pinning sites of magnetic domains and enhance the internal demagnetization field of Fe-based soft magnetic composites, thus increasing the difficulty of domain wall displacement and domain flipping.

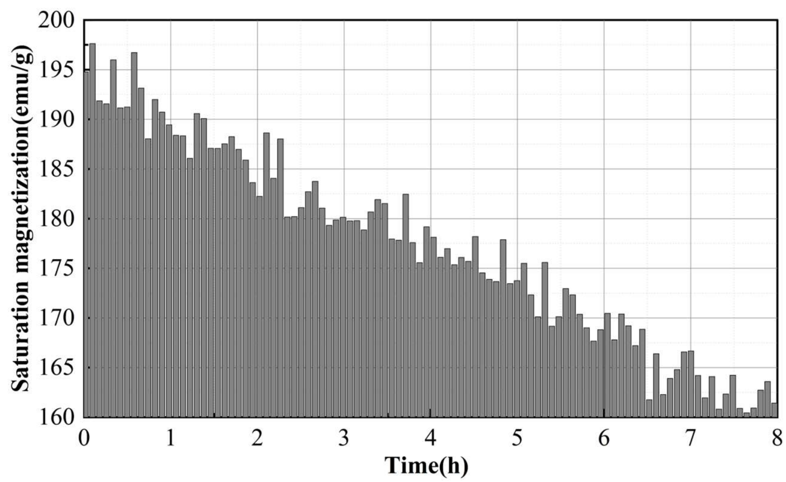

Fig. 4. The magnetization intensity of the materials under different oxidation time

The results of density, resistivity and magnetic loss measurements of Fe-based soft magnetic composites at different oxidation times are shown in Table 1. The decrease with the increase of oxidation time is attributed to the increase of the insulating layer content of the relatively low density Fe-based soft magnetic composites. When the oxidation time is increased from 0h to 8h, the resistivity of the Fe-based soft magnetic composites shows a tendency of increasing and then decreasing. It is noteworthy that the resistivity is very low (2.59 $m\Omega \cdot cm$ and 5.48 $m\Omega \cdot cm$) when the oxidation time is below 0.5h. When the oxidation time was increased to 1h, the resistivity increased significantly (161.60 $m\Omega \cdot cm$). When the oxidation time reaches 2h, the resistivity gets a relative maximum (384.74 $m\Omega \cdot cm$). When the oxidation time continues to increase, a paradoxical decrease in resistivity occurs. When the oxidation time is lower than 0.5h, the resistivity of the samples with oxidation times of 0h and 0.5h is low due to the existence of local inhomogeneity in the insulating layer of the Fe-based soft magnetic composites, which results in the direct contact of the ferrous alloy cores, which is not conducive to the inter-particle insulation, and therefore the resistivity is low, and the resistivity is slightly elevated with the increase of the oxidation time. When the oxidation time reaches 1h, the oxide layer completely covers the surface of the ferroalloy powder, and the uniformity and thickness of the insulating layer of Fe-based soft magnetic composites are improved, which can effectively impede the movement of free electrons between particles, and thus the resistivity is significantly improved. With the increase of oxidation time to 2h, the thickness of the insulating layer of Fe-based soft magnetic composites increased, which led to the increase of resistivity. Combining the above results and analysis, when the oxidation time is short, the resistivity of Fe-based soft magnetic composites is mainly affected by the uniformity of the insulating layer of Fe-based soft magnetic composites. When the oxidation time is moderate, the resistivity of Fe-based soft magnetic composites is mainly affected by the thickness of the insulating layer of Fe-based soft magnetic composites. When the oxidation time is too long, the resistivity of the Fe-based soft magnetic composites is mainly affected by the intrinsic resistivity of the ferroalloy core and the in-situ Fe content in the insulating layer of the Fe-based soft magnetic composites. In addition, under the test condition of 50 mT/100 kHz, when the oxidation time is gradually increased from 0 h to 8 h, the magnetic loss first decreases significantly and then continues to increase, and the sample with an oxidation time of 2 h exhibits the relatively lowest magnetic loss (215.63 mW/cm^3).

Table 1. Density, resistivity and magnetic loss of material with different oxidation time

Oxidation time (h)	Density (g/cm^3)	Resistivity ($m\Omega \cdot cm$)	Magnetic loss (mW/cm^3)		
			20 mT/20 kHz	50 mT/20 kHz	50 mT/100 kHz
0	7.09	2.59	40.51	265.56	2893.57
0.5	7.09	5.48	27.8	231.39	2668.86
1.0	7.08	161.60	21.99	105.26	592.63
1.5	7.06	315.34	10.42	42.56	322.65
2.0	7.04	384.74	6.80	38.52	215.63
2.5	7.00	379.52	4.02	45.17	258.12
3.0	7.00	354.62	4.29	50.30	282.94
3.5	6.99	332.65	4.74	56.11	378.47
4.0	6.99	330.15	5.71	56.16	454.25
4.5	6.96	329.65	5.75	64.58	544.90
5.0	6.89	324.52	9.02	65.47	606.09
5.5	6.86	315.26	9.48	69.63	626.74
6.0	6.86	305.47	12.17	73.04	689.48
6.5	6.82	304.38	12.34	81.73	698.43
7.0	6.78	277.94	12.62	83.34	901.50
7.5	6.69	221.86	12.72	89.71	1025.30
8.0	6.62	209.91	14.23	90.85	1089.80

4.3. Optimization analysis of vibration noise of core reactor

The saturation magnetization strength and magnetic loss of Fe-based soft magnetic composites will have an impact on the vibration of the core reactor, and this study analyzes the vibration of the core reactor with different parameters by adjusting the oxidation time parameter of Fe-based soft magnetic composites in a three-dimensional finite element model. From the above analysis of the performance of Fe-based soft magnetic composites under different parameter conditions, it can be seen that the oxidation time of this parameter condition for 0h, 2h and 8h when the material performance will appear a big difference, so this paper selected these three parameter conditions for simulation and analysis.

In order to ensure that the simulation experiment conditions are consistent with the previous simulation accuracy verification conditions, the vibration sensor is used to measure the core, clamps, nuts and windings on the reactor at 4 points. The amplitudes of the three points of vibration measurement were obtained when the oxidation time parameters of Fe-based soft magnetic composite materials were 0h, 2h and 8h, respectively. The comparison curves of the vibration displacement velocity of the core reactor with different oxidation times are shown in Fig. 5, and (a)-(d) represent the measurement results of the core, clamp, nut and winding at four points, respectively. The calculation results of the vibration reduction effect are shown in Table 2. Different oxidation time parameters Fe-based soft magnetic composite iron core reactor vibration displacement velocity at each point there is a significant difference between the 2h and 8h oxidation time relative to the un-oxidized Fe-based soft magnetic composite iron core reactor vibration displacement velocity are significantly reduced, effectively proving the correctness of the theoretical analysis, which also proves that the parameter change and optimization for the vibration damping of the iron core reactor is feasible. This also proves that the change and optimization of this parameter is feasible for the vibration reduction of core reactor. From the results of the vibration displacement velocity analysis, it can be seen that the average vibration displacement velocity of the core, clamp, nut and winding of the Fe-based soft magnetic composite core reactor with an oxidation time of 0 h is 0.307 mm/s, 0.225 mm/s, 0.223 mm/s and 0.146 mm/s. The average vibration displacement velocity of the Fe-based soft magnetic composite core reactor with 2 h oxidation time is the lowest, which is 0.17 mm/s. The average vibration displacement velocity is the lowest, which is 0.17 mm/s, respectively. velocity is the lowest, which is 0.176mm/s, 0.155mm/s, 0.097mm/s and 0.043mm/s, respectively, and the vibration reduction amplitude is in the range of 31.11%~70.55%, which proves that there is a good effect of vibration reduction and noise reduction of the reactor under the material parameters.

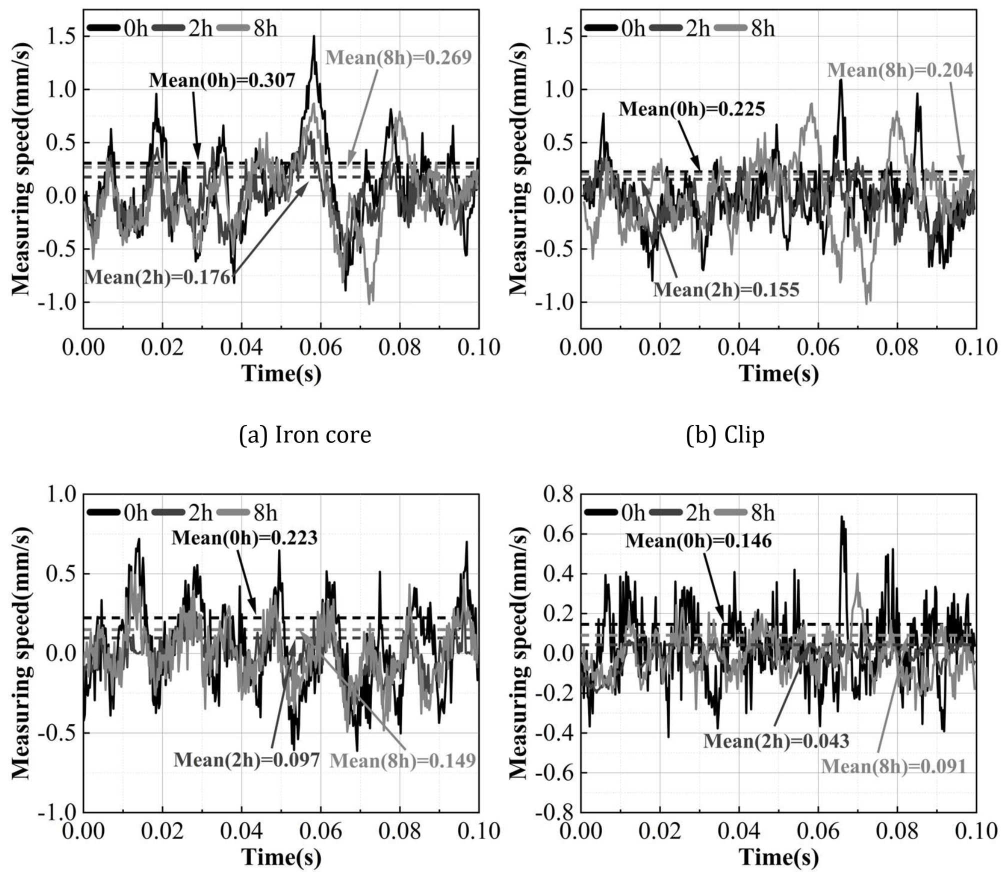

(a) Iron core (b) Clip

(c) Nut (d) Winding

Fig. 5. Vibration analysis of iron core reactor of different oxidation time materials

Table 2. Analysis of vibration reduction effect

Damping effect		Vibration point			
		Iron core	Clip	Nut	Winding
Vibration displacement velocity (mm/s)	0h	0.307	0.225	0.223	0.146
	2h	0.176	0.155	0.097	0.043
	8h	0.269	0.204	0.149	0.091
Reduction amplitude	2h VS 0h	42.67%	31.11%	56.50%	70.55%
	8h VS 0h	12.38%	9.33%	33.18%	37.67%

5. Conclusion

This paper combines the basic parameters of Fe-based soft magnetic composite core reactor, in ANSYS Maxwell software to establish a three-dimensional finite element analysis model of the core reactor, through experiments to verify the simulation accuracy of the finite element model, and found that the core reactor core, clamps and winding vibration sampling points of the simulation simulation results and the measured results of the peak of the time domain waveforms and the rule of change is relatively close. At the same time, it is found that the relative error of the main vibration frequency amplitude of the reactor is less than 5%, indicating that the model has accuracy and feasibility.

According to the Fe-based soft magnetic composites performance measurement method simulation analysis of different oxidation parameters under the material saturation magnetization strength and magnetic loss and other parameters, found that the material saturation magnetization strength with the increase of oxidation time and reduce, but the magnetic loss with the increase in oxidation time shows the first decrease and then increase the trend, oxidation time of 2h when the magnetic loss of the lowest for 215.63 mW/cm^3 . The simulation analysis of the optimization effect of different parameter materials on the vibration damping of the core reactor reveals that the average vibration displacement velocity of Fe-based soft magnetic composite core reactor is the lowest under 2h oxidation time, and the vibration damping amplitude is 31.11%~70.55% relative to the unoxidized material.

In conclusion, this study verifies the feasibility of changing the oxidation parameters of Fe-based soft magnetic composites for the optimization of vibration reduction of the core reactor through simulation analysis, which provides a new method for vibration and noise reduction of this type of reactor.

Funding

This work was supported by State Grid Hebei Electric Power Co., Ltd. Science and technology project funding: A new type of low noise core reactor based on Fe-based soft magnetic composite material is developed (5204CZ240002).

References

[1] Wang, Z., Yu, R., Duan, C., Fan, Z., & Li, X. (2023, September). Analysis of the Vibration Characteristics and Vibration Reduction Methods of Iron Core Reactor. In Actuators (Vol. 12, No. 9, p. 365). MDPI.

[2] Pfeifer, N., Kizilcay, M., & Malicki, P. (2023). Analytical and numerical study of an iron-core shunt-compensation reactor on a mixed transmission line. Electric Power Systems Research, 220, 109315.

[3] Gao, L., Ji, S., Zhu, L., Yang, H., Zhang, F., Li, J., & Hui, S. (2021). Vibration and noise characteristics of air-core reactor used in HVDC converter stations. IEEE Transactions on Power Delivery, 37(2), 1068-1077.

[4] Zhang, P., Li, L., Cheng, Z., Tian, C., & Han, Y. (2018). Study on vibration of iron core of transformer and reactor based on maxwell stress and anisotropic magnetostriction. IEEE Transactions on Magnetics, 55(2), 1-5.

[5] Zhao, C., Pang, W., Han, K., Xie, B., & Guo, H. (2020, October). Study on The Characteristics of Reactor Core Vibration Acoustic Signal under Different Excitation. In 2020 IEEE 4th Conference on Energy Internet and Energy System Integration (EI2) (pp. 1131-1136). IEEE.

[6] Gao, Y., Ichimaru, S., Miyabe, T., Dozono, H., Muramatsu, K., Guan, W., ... & Chen, B. (2020). Proposal of core structures for iron loss and noise reduction of three-phase reactor with anisotropic iron core. IEEE Transactions on Magnetics, 57(2), 1-5.

[7] Yuan, F., Lv, K., Tang, B., Wang, Y., Yang, W., Qin, S., & Ding, C. (2021). Optimization Design of Oil-Immersed Iron Core Reactor Based on the Particle Swarm Algorithm and Thermal Network Model. Mathematical problems in Engineering, 2021(1), 6642620.

[8] Yuan, J., Li, X., Mo, Z., & Ji, Y. (2022). Research on vibration of the reactor for HVDC thyristor protection. Energy Reports, 8, 321-329.

[9] Liu, J., & Zhao, Y. (2022, December). Temperature field analysis of dry iron core reactor. In Journal of Physics: Conference Series (Vol. 2401, No. 1, p. 012022). IOP Publishing.

[10] Yao, A., Tsukada, K., Odawara, S., Fujisaki, K., Shindo, Y., Yoshikawa, N., & Yoshitake, T. (2017). PWM inverter-excited iron loss characteristics of a reactor core. AIP Advances, 7(5).

[11] Yan, R., Gao, X., Zhu, L., Yang, Q., Ben, T., Li, Y., & Yang, W. (2016). Research on three-dimensional stress distribution of reactor core. IEEE Transactions on Applied Superconductivity, 26(4), 1-4.

[12] Tong, B., Qingxin, Y., Rongge, Y., & Lihua, Z. (2017). Magnetically controlled saturable reactor core vibration under practical working conditions. IEEE Transactions on Magnetics, 53(6), 1-4.

[13] Li, Y., Liu, Y., Li, S., Qi, L., Xie, J., & Xie, Q. (2022). A novel multi-objective optimal design method for dry iron core reactor by incorporating NSGA-II, TOPSIS and entropy weight method. Energies, 15(19), 7344.

[14] Liao, C., Liu, B., Li, K., & Wang, W. (2024). Accuracy improvement of thermal distribution analysis of 10 kV dry-type iron-core reactor. Case Studies in Thermal Engineering, 64, 105554.

[15] Younes Mehrifar,Hamed Moqtaderi,Seyedeh Mehri Hamidi,Farideh Golbabaei,Mahdi Hasanzadeh & Somayeh Farhang Dehghan. (2025). Magnetic nanoparticles of Nd2Fe14B prepared by ethanol-assisted wet ball milling technique. Scientific reports(1),3257.

[16] Yi Xuwu,Peng Yuandong,Yao Zhixin,Xia Chao & Zhu Shengzhi. (2021). Microstructure and magnetic properties of FeSiAl soft magnetic composites prepared by chemical in-situ coprecipitation with NaOH. Materials Chemistry and Physics.

[17] Huanan Wei & Xudong Wang. (2025). Effect of opening auxiliary slots in the primary of permanent magnet synchronous linear motors on magnetic resistance. Journal of Physics: Conference Series(1),012003-012003.

[18] Chengzhuo Zhao,Wenjie Tang,Kangshuai Du & Na Liu. (2025). Symplectic mixed spectral element time domain method for 3-D Schrödinger–Maxwell equations under Lorenz gauge. Applied Mathematics Letters109497-109497.

[19] Wang Tingting,Zheng Changbao,Zhou Rui,Wang Qunjing,Ju Lufeng & He Jingxiong. (2021). Research on torque analytical model of permanent-magnet spherical motor based on torque map by Lorentz force method. International Journal of Applied Electromagnetics and Mechanics(4),735-752.